

News from LHC: Recent Results on Higgs Physics

A. Straessner*, on behalf of the ATLAS Collaboration

Technische Universität Dresden, Dresden

E-mail: Arno.Straessner@tu-dresden.de

The ATLAS and CMS experiments at the LHC have measured detailed properties of the SM-like Higgs boson discovered in 2012. Results on Higgs boson mass, width, spin and coupling determinations are presented. The parameters observed are furthermore interpreted in extensions to the Standard Model. Searches for additional Higgs bosons predicted in the general 2 Higgs Doublet Model (2HDM) and the Minimal Supersymmetric Standard Model (MSSM) are reported.

Frontier Research in Astrophysics

26 - 31 May, 2014

Mondello (Palermo), Italy

*Speaker.

1. Introduction

The Large Hadron Collider (LHC) [1] is a proton-proton (pp) collider which has been operated in 2011 and 2012 at centre-of-mass energies, \sqrt{s} , of 7 TeV and 8 TeV, respectively. One of the primary goals of the LHC physics programme is the exploration of the Higgs mechanism and the study of mass generation of elementary particles by electro-weak symmetry breaking. The main signature of a mass generating Higgs field predicted by the Standard Model (SM) [4] is a scalar Higgs boson with well defined properties: its spin-CP structure should be $J^{\text{CP}} = 0^{++}$ and it should couple to all heavy gauge bosons and elementary fermions proportional to their mass. With about $2 \times 5 \text{ fb}^{-1}$ of data of the first LHC physics run (Run-1) the ATLAS and CMS Collaborations [2, 3] had both measured a significant excess of candidate events from Higgs boson production and decay above the background expectation. This finally led to announcements of the observation of a scalar Higgs boson [5]. Nearly the complete Run-1 data set of about $2 \times 26 \text{ fb}^{-1}$ has now been analysed to further study the detailed properties of the Higgs boson, in particular its mass, width, coupling structure, as well as spin and CP properties.

Several reasons lead to the assumption that the Standard Model may however not be valid at energy scales up to the Planck scale, like e.g. the observation of Dark Matter in the Universe. This phenomenon may be explained by additional weakly interacting massive particles which are not part of the Standard Model. Extensions of the Standard Model are therefore also tested at the LHC. Possible signatures are an extended Higgs sector [20], like the 2 Higgs Doublet Model (2HDM), of which the Minimal Supersymmetric Standard Model (MSSM) is a special realisation.

This article summarizes the most recent experimental results by ATLAS and CMS on the search and measurement of a SM-like Higgs boson, the determination of its properties and searches for Higgs bosons beyond the SM.

2. Search for the Standard Model Higgs Boson

In pp collisions at 7-8 TeV centre-of-mass energy, the main production channel of the Standard Model Higgs boson with a mass around 125 GeV is gluon-gluon fusion (87%), where gluons inside the protons interact indirectly via a top-quark loop with the Higgs boson. The search must therefore rely on identifying specific Higgs boson decay modes. Additional final state signatures can be utilized in other production channels. In vector-boson-fusion (VBF, 7%) the Higgs boson decay is accompanied by a pair of jets. In associated Higgs boson production with a W boson or Z boson (5%) and in associated production with a pair of top quarks (1%), the corresponding decay products of W and Z bosons or top quarks can be used to distinguish the SM Higgs boson signal from background. The different production cross-sections for a SM Higgs boson mass of 125 GeV are shown in Figure 1 [6] as function of centre-of-mass energy.

The main decay modes which are analysed in the SM Higgs boson searches are the $H \rightarrow \gamma\gamma$ and the $H \rightarrow ZZ^* \rightarrow \ell^+\ell^-\ell^+\ell^-$ channels, where the lepton pairs, $\ell^+\ell^-$, are either an electron and a positron or a pair of oppositely charged muons. The corresponding branching ratios are compared to each other in Figure 1. Since the final state photons, electrons and muons can be reconstructed with excellent energy and momentum resolution, the invariant mass spectrum of the Higgs boson candidates is used to discriminate between signal and the SM background processes. In the data

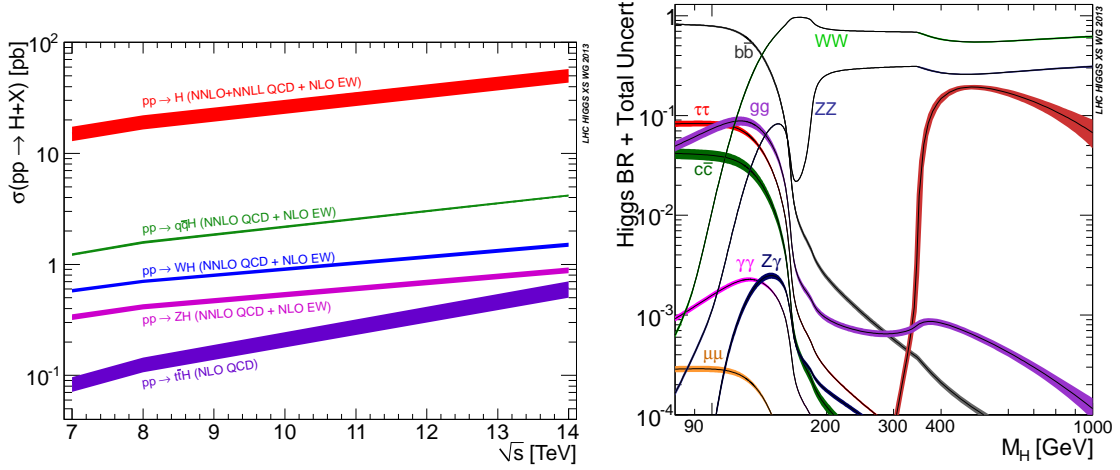


Figure 1: SM predictions of Higgs boson production cross-sections (left) for pp collisions at $\sqrt{s} = 7 - 14$ TeV and of Higgs branching fractions for Higgs boson masses, m_H , between 90 GeV and 1 TeV (right).

Table 1: Observed and expected statistical significance of the hypothesis that the data is compatible with a SM background fluctuation, corresponding to the minimal local p_0 value, for the SM Higgs boson searches in bosonic and fermionic decay channels [7].

Experiment	Statistical significance (σ)							
	$H \rightarrow ZZ$		$H \rightarrow \gamma\gamma$		$H \rightarrow W^+W^-$		$H \rightarrow \tau^+\tau^-$	
	obs.	exp.	obs.	exp.	obs.	exp.	obs.	exp.
ATLAS	6.6	4.4	7.4	4.3	3.8	3.8	4.1	3.2
CMS	6.8	6.7	3.2	4.2	4.3	5.8	3.2	3.7

analysed, an excess of data above SM background expectation is observed in both channels and by both, ATLAS and CMS, in the invariant mass ranges around 125-126 GeV, as shown in Figure 2. The observed local probabilities, p_0 , that the data are compatible with fluctuations of the estimated background can be expressed in terms of statistical significances, σ , and are summarized in Table 1. In all channels in which the Higgs boson decays into a pair of gauge bosons, including the $H \rightarrow W^+W^- \rightarrow \ell\nu\ell\nu$ final state, a clear Higgs boson signal is observed [7].

Within the SM, the Higgs boson does not couple directly to massless gluons and photons. Therefore, Higgs boson production in gluon-gluon fusion and decay to a pair of photons are mediated by loop diagrams involving massive fermions. The observation of a Higgs boson signal is therefore an indication that the Higgs-fermion coupling has also non-zero strength. Up to the time of the conference, a direct Higgs boson decay to fermion pairs has been observed with significances above 3σ in the $H \rightarrow \tau^+\tau^-$ channel [8], only (see Table 1). Both hadronic and leptonic decays of tau leptons were analysed to identify the $H \rightarrow \tau^+\tau^-$ decay.

More complex final states, like $W/Z + H$ with $H \rightarrow b\bar{b}$, have been searched for, but do not yet yield clear evidence for a Higgs boson signal [9]. The rare production mode $t\bar{t}H$ with $H \rightarrow$

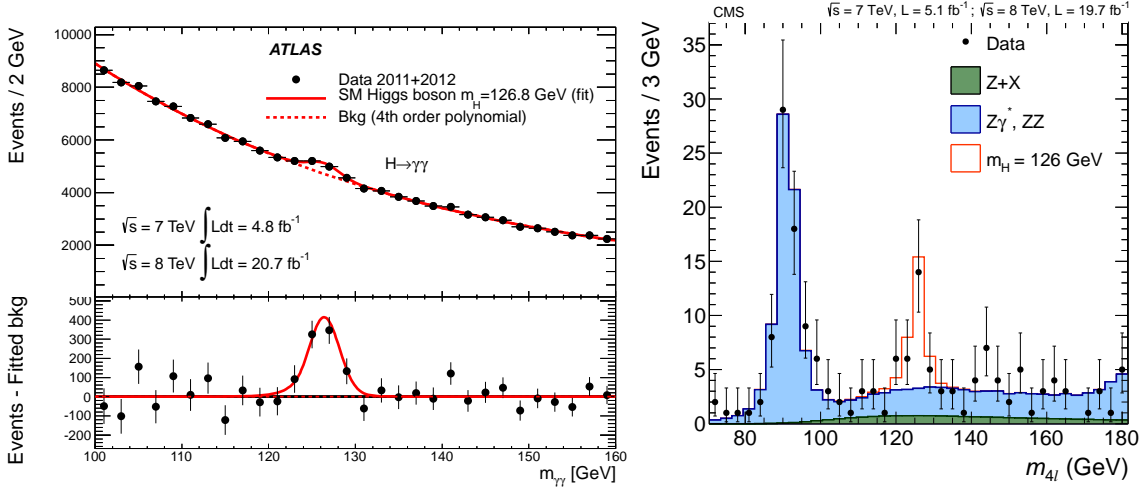


Figure 2: Examples of di-photon (left) and four lepton (right) invariant mass spectra measured for SM Higgs boson candidates, as determined by ATLAS and CMS, respectively [7]. The red curves show a SM Higgs signal prediction for a Higgs mass of 126 GeV above the background expectation.

$\gamma\gamma, W^+W^-, ZZ, \tau^+\tau^-, b\bar{b}$ is particularly interesting because the Higgs boson Yukawa coupling to the top quark, y_t , which is proportional to the ratio of the top quark mass, m_t , and the Higgs vacuum expectation value, v , reaches values close to one: $y_t = \sqrt{2}m_t/v \approx 1$. However, more data are needed to improve on the results, which yield ratios of measured cross-section to SM expectation of $\mu = \sigma/\sigma_{\text{SM}} = 1.7 \pm 1.4$ and $\mu = 2.5^{+1.1}_{-1.0}$ [10] for ATLAS and CMS, respectively.

The ratio μ is used to compare the signal strengths in all Higgs boson decay channels to the SM prediction. An example for individual measurements by CMS is given in Figure 3 [9]. The combined μ values derived by CMS and ATLAS are $\mu = 0.80 \pm 0.14$ and $\mu = 1.30^{+0.18}_{-0.17}$, respectively. Overall, a good agreement to the SM expectation $\mu_{\text{SM}} = 1$ is observed.

3. Higgs Boson Properties

The main Higgs boson characteristics which have been determined in LHC Run-1 are the coupling strength to fermions and bosons, its mass and width, and its spin and CP parameters.

At the LHC, only the product of cross-section, $\sigma_i = \sigma(i \rightarrow H)$, and branching ratio, $\text{BR}(H \rightarrow f)$, with initial state i and final state f can be measured. In the narrow Higgs width approximation, this product is expressed as $\sigma \times \text{BR}(i \rightarrow H \rightarrow f) = \sigma_i \Gamma_f / \Gamma_H$, where Γ_f and Γ_H are the partial and total width of the Higgs boson. In order to extract the Higgs boson coupling strength to other particles, the cross-section and partial widths are assumed to scale with coupling parameters κ_j according to $\sigma_j = \kappa_j \sigma_{j,\text{SM}}$ and $\Gamma_j = \kappa_j \Gamma_{j,\text{SM}}$. Furthermore, it is assumed that the Lorentz structure of the fermion and vector boson couplings to the Higgs boson is realised as in the SM. For loop-induced production and decay modes, $gg \rightarrow H$ and $H \rightarrow \gamma\gamma$, interference effects are taken into account [9]. It is furthermore assumed that only SM particles contribute to the total width and that fermion and vector boson couplings scale with common factors κ_F and κ_V , respectively. Limits in the κ_F vs. κ_V plane are extracted and shown in Figure 3 for ATLAS, while CMS findings are very

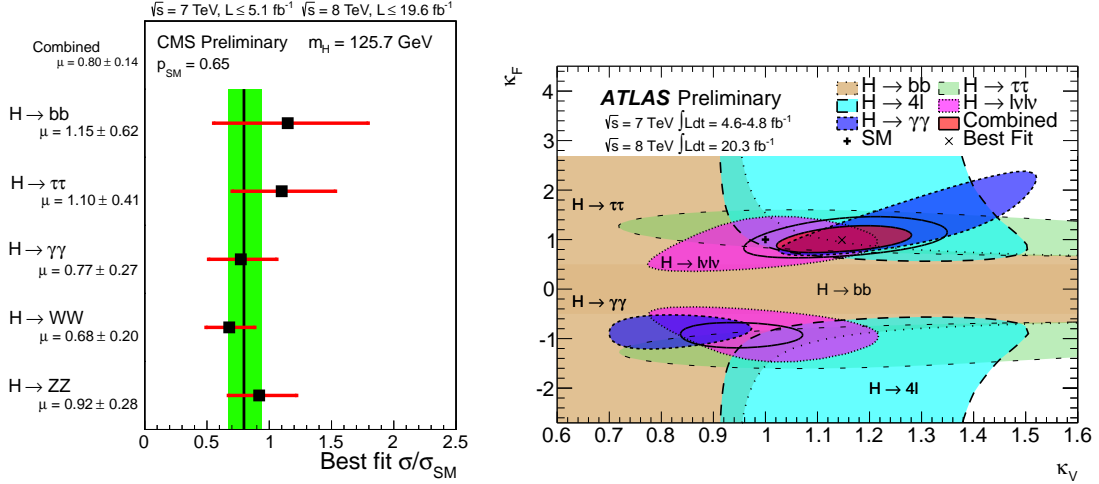


Figure 3: Left: Signal strength parameter $\mu = \sigma/\sigma_{SM}$ for individual Higgs boson decay channels measured by CMS [9]. Right: fermionic and bosonic Higgs boson coupling parameters, κ_F and κ_V , derived by ATLAS [9].

similar [9]. One can observe that the combined coupling strengths are well compatible with the SM value of 1. Furthermore, the sign ambiguity in the fermionic coupling is resolved by interference terms, which are linear in κ_j , such that the combined fermionic coupling is found to be positive, as predicted in the SM.

Another interesting test concerns the ratio $\lambda_{WZ} = \kappa_W/\kappa_Z$ of the W and Z boson couplings to the Higgs boson. In the SM, this coupling ratio is protected by the so-called custodial SU(2) symmetry, which leads to a coupling ratio of 1 at lowest order with small higher order corrections of the size m_b/m_t . The ATLAS and CMS measurements show values of $\lambda_{WZ} = 0.94^{+0.14}_{-0.29}$ and $\lambda_{WZ} \in [0.7, 1.0]$ at 68% confidence level (CL) which are consistent with $\lambda_{WZ}^{SM, tree-level} = 1$ within the still large uncertainties.

In the coupling strength analyses, the SM coupling structure is assumed, which is related to the spin and CP properties of the Higgs boson. According to the Landau-Yang theorem [11], the spin-1 hypothesis for the newly observed state is excluded by observing its decay into a pair of real photons, $H \rightarrow \gamma\gamma$. To analyse further Higgs boson properties, angular distributions of the final state particles in $H \rightarrow \gamma\gamma$, $H \rightarrow W^+W^- \rightarrow l^+ \nu l^- \bar{\nu}$ and $H \rightarrow ZZ \rightarrow l^+ l^- l^+ l^-$ events are used to discriminate between different spin and CP hypotheses. Figure 4 shows, as an example, the distribution of the cosine of the angle between the decay planes of the two Z bosons in $H \rightarrow ZZ$ candidate events, reconstructed from the four leptons in the final state. The relatively small discrimination power of a single variable, to distinguish e.g. between a $J^P = 0^+$ and a $J^P = 0^-$ state, can be enhanced by multivariate techniques. On the right-hand side of Figure 4, the output of a Boosted Decision Tree (BDT [12]) analysis performed by ATLAS is shown. Using such techniques, the ATLAS and CMS analyses show that the $J^P = 0^+$ nature of the Higgs boson is favoured with respect to other models, and spin-2 models are disfavoured at more than 95% CL [13].

Unlike spin and CP properties and the fermionic and bosonic coupling strengths, the mass of the Higgs boson, m_H , is not predicted by the SM. Like all particle masses in the SM, the value of

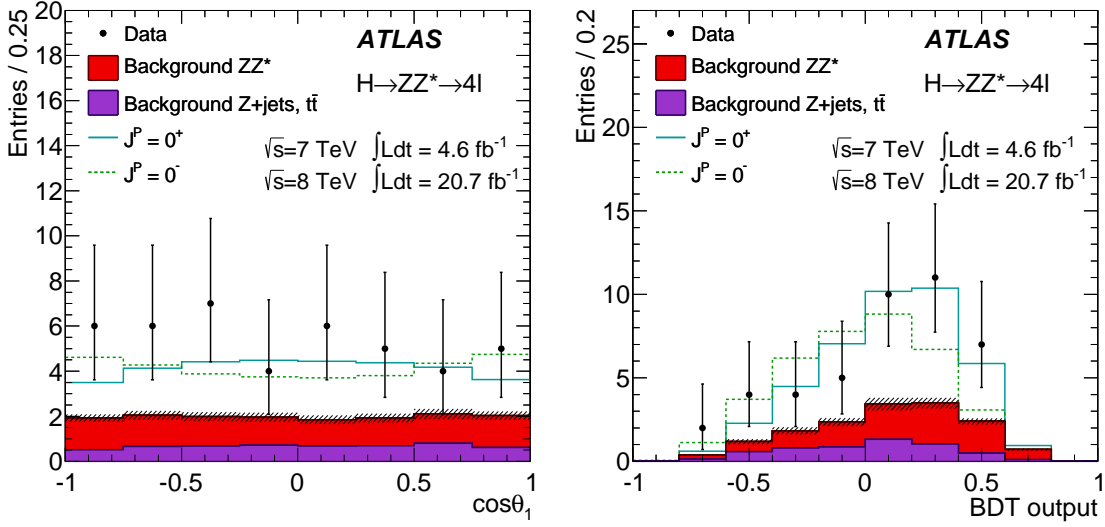


Figure 4: The distribution of the cosine of the angle between the Z decay planes in $H \rightarrow ZZ \rightarrow \ell^+ \ell^- \ell^+ \ell^-$ events (left) is one of the input variables to the BDT analysis (right) by ATLAS [13]. Additional information on the spin and CP properties of the Higgs boson is contained in the decay angle of the leptons in the Z rest frames, which serve as Z polarimeter, and in the invariant mass distributions of the lepton pairs.

m_H is proportional to the Higgs vacuum expectation value $v \approx 246$ GeV [14]. However, it also depends on the Higgs boson self-coupling strength, λ , which is a free parameter of the SM Higgs potential. With the observation of the new scalar resonance, also m_H can now be determined from the invariant mass spectra in the decays $H \rightarrow \gamma\gamma$ and $H \rightarrow ZZ \rightarrow \ell^+ \ell^- \ell^+ \ell^-$. These channels provide excellent mass resolution of the order of 1-2%. In order to improve the sensitivity on m_H , the data are categorized according to their invariant mass resolution. The Higgs mass parameter is then extracted from one- or multi-dimensional fits to invariant mass spectra including background parameterisations. The systematic uncertainties in the $H \rightarrow \gamma\gamma$ channel are dominated by the photon energy scale of the electromagnetic calorimeters, and in the $H \rightarrow ZZ$ channel by the muon momentum calibration since the 4-muon final state has the greatest sensitivity to m_H among the different $H \rightarrow ZZ$ channels. These energy and momentum scales are calibrated using large statistics control samples of well-known resonance decays like $Z \rightarrow e^+ e^-$ for the electromagnetic energy measurement and $J/\psi \rightarrow \mu^+ \mu^-$, $\Upsilon \rightarrow \mu^+ \mu^-$, $Z \rightarrow \mu^+ \mu^-$ for the muon momentum scale. The ATLAS and CMS results after combining the Higgs boson decay channels yield [15]:

$$m_H = 125.7 \pm 0.3 \text{ (stat.)} \pm 0.3 \text{ (syst.) GeV (CMS)} \quad (3.1)$$

$$m_H = 125.5 \pm 0.2 \text{ (stat.)} {}^{+0.5}_{-0.6} \text{ (syst.) GeV (ATLAS)}. \quad (3.2)$$

The resonance shape can also be used to derive a measurement of the Higgs boson width. In the SM, the Higgs boson width is narrow with a value of $\Gamma_H = 4.2$ MeV [14]. Due to the limited invariant mass resolution, a direct determination of the Higgs boson width by the CMS Collaboration yields upper limits of $\Gamma_H < 3.4$ GeV at 95% CL [7]. An indirect method was proposed [16] to

circumvent the resolution constraint by exploiting the off-shell behaviour of the Breit-Wigner resonance. In the narrow width approximation, the off-peak differential resonance cross-section scales with respect to the peak cross-section proportional to the Higgs boson width: $\sigma_{\text{off-peak}}/\sigma_{\text{peak}} \propto \Gamma_H$. The CMS analysis of the $gg \rightarrow H \rightarrow ZZ$ channel takes interference effects with the ZZ continuum and a variation of the $gg \rightarrow H$ signal strength as well as the VBF signal strength into account. The observed off-peak spectrum agrees with SM expectations. It is thus interpreted as a determination of the Higgs boson width obtaining $\Gamma_H = 1.8_{-1.8}^{+7.7}$ MeV, respectively an upper limit of $\Gamma_H < 22$ MeV at 95% CL [17]. The indirect Higgs boson width measurement is thus in agreement with SM predictions.

The total Higgs boson width may still have contributions from invisible decays. These would manifest both in a measurable cross-section of the VBF and ZH processes, with $H \rightarrow$ invisible, and in a modified total Higgs boson width. The latter then scales with respect to the SM prediction according to [18]:

$$\kappa_h = \frac{\Gamma_H}{\Gamma_{H,\text{SM}}} = \frac{0.0023\kappa_\gamma + 0.098\kappa_g + 0.91}{1 - \text{BR}_i}, \quad (3.3)$$

where BR_i is the Higgs boson branching ratio to invisible particles. Using the Higgs boson coupling measurements and the upper limits on the VBF- $H \rightarrow$ invisible and $ZH \rightarrow \ell^+\ell^- +$ invisible production cross-sections, the invisible Higgs boson branching ratio is constrained by ATLAS and CMS to $\text{BR}_i < 0.37$ and $\text{BR}_i < 0.58$, respectively, at 95% CL [18]. This can be interpreted further in a scenario where the Higgs boson couples to Weakly Interacting Massive Particles (WIMP), χ , which may be a candidate for Dark Matter (DM) in the Universe. Assuming that the invisible partial width, $\Gamma_i(H \rightarrow \chi\chi)$ and the WIMP-nucleon cross-section, $\sigma_{\chi-N}$, both scale with a common parameter $\lambda_{h\chi\chi}$ [18]:

$$\Gamma_i(H \rightarrow \chi\chi) \propto \lambda_{h\chi\chi}^2 \quad \sigma_{\chi-N} \propto \lambda_{h\chi\chi}^2 \quad (3.4)$$

one can derive upper limits on $\sigma_{\chi-N}$ as a function of the WIMP mass, m_χ , up to the kinematic limit $m_\chi < m_H/2$. The results are displayed in the $\sigma_{\chi-N}-m_\chi$ plane for the CMS measurement [18] in comparison with direct WIMP searches. ATLAS obtains very similar upper limits. Depending on the spin of the WIMP, the LHC is in particular sensitive in the low WIMP mass region, within the scenario assumed here, and thus complementary to direct DM searches.

4. Search for Higgs Bosons Beyond the Standard Model

The SM Higgs sector can be considered minimal in the sense that the Higgs field provides gauge invariant mass terms for gauge bosons and fundamental fermions, and the only additional physical excitation of the Higgs field is the massive Higgs boson. Up to now, this model is in agreement with observation, also fulfilling constraints from electro-weak precision physics, like the so-called ρ parameter, which receives a value of 1 at tree level [4]. This leading order condition remains valid if multiple $\text{SU}(2)_L$ Higgs doublets are added to the theory [19]. One possible SM extension is therefore the 2 Higgs Doublet Model (2HDM [20]), in which each Higgs doublet field, Φ_1 and Φ_2 , obtains a vacuum expectation value, v_1 and v_2 . These are related to the SM vacuum expectation value by $v_1^2 + v_2^2 = v^2 \approx (246 \text{ GeV})^2$, and their ratio is typically parameterized by $\tan\beta = v_2/v_1$.

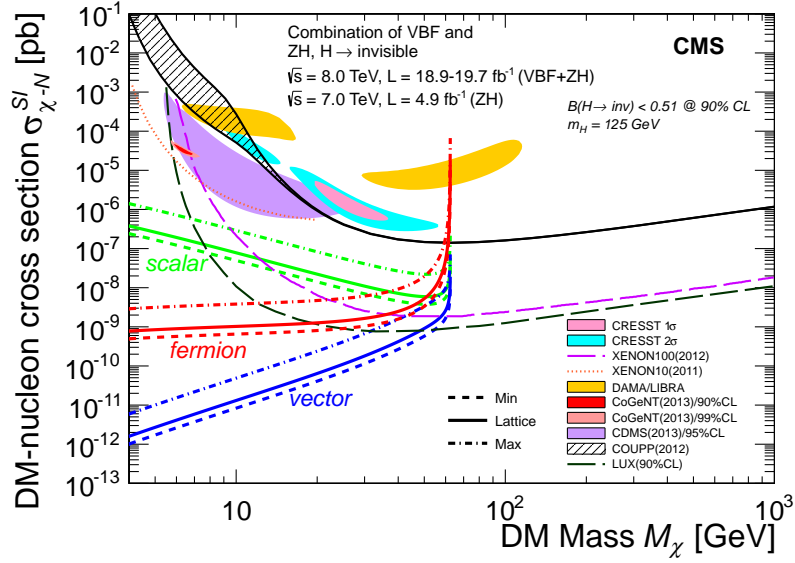


Figure 5: Upper limits on the Dark Matter (DM) nucleon cross-sections determined from the invisible Higgs boson decay width by the CMS experiment compared to direct DM search results [18].

The physical states are 5 Higgs bosons: 2 neutral CP-even states, h and H , which are usually ordered by mass, $m_h < m_H$, 1 neutral CP-odd state, A , and 2 charged states, H^\pm . The CP-even Higgs bosons are obtained from a mixing of the fundamental Higgs field components with a mixing angle α . This angle and the parameter β enter the coupling scale factors of the neutral CP-even Higgs boson, h , to the heavy vector bosons (κ_V), the up- and down-type quarks (κ_u , κ_d) and the leptons (κ_l). These are summarized in Table 2 for the four different types of 2HDM scenarios [20]:

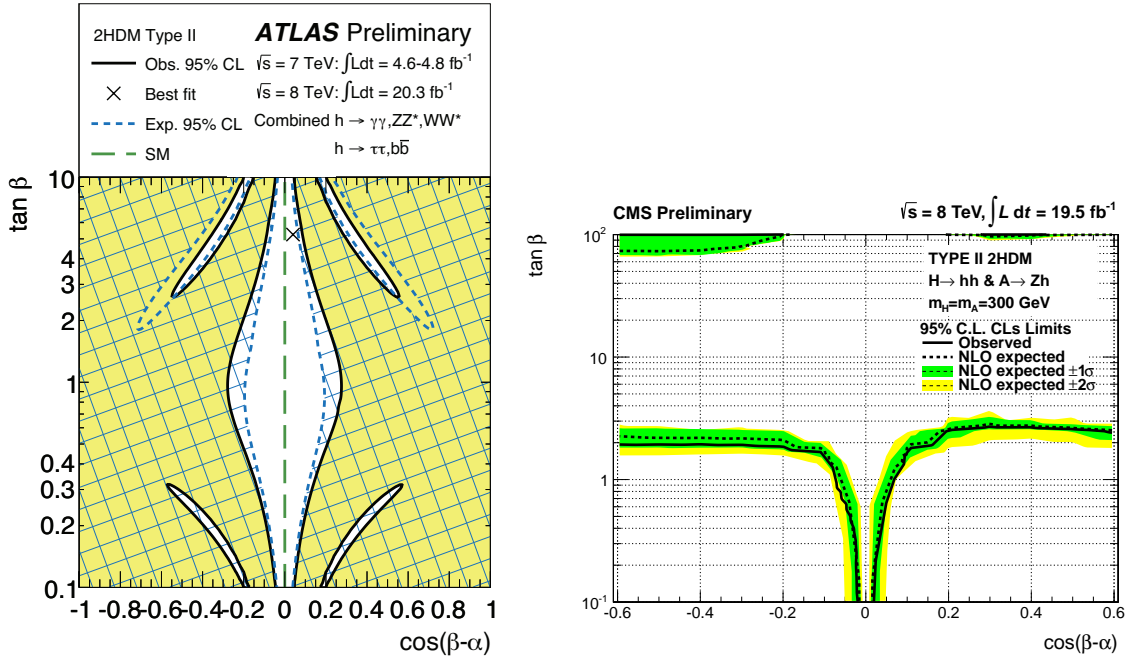
- Type I: Φ_1 couples only to fermions and Φ_2 only to gauge bosons; in absence of mixing between the fields, one can construct a “fermiophobic” scenario, where h does couple to fermions weakly
- Type II: Φ_1 couples to down-type fermions and Φ_2 only to up-type fermions; the Minimal Supersymmetric Standard Model (MSSM) requires this 2HDM realisation
- Type III: one doublet with quark couplings like in Type I, the other with lepton couplings like in Type II; also called “lepton-specific” scenario
- Type IV: lepton and quark couplings opposite to Type III; the “flipped” scenario

The fermionic and bosonic coupling strength measurements of the newly discovered neutral Higgs boson can thus be interpreted in the 2HDM scenarios in order to constrain the model parameters α and β . Figure 6 shows the excluded parameter space in the $\tan\beta$ vs. $\cos(\beta - \alpha)$ plane within the Type-II 2HDM. The allowed regions include the SM parameter value $\cos(\beta - \alpha) = 0$ for any $\tan\beta$, indicating that the CP-even Higgs boson appears to be SM-like. A similar behaviour is found for the other 2HDM scenarios of Type I, III, and IV [21].

The additional and usually heavier Higgs bosons, H and A , are also searched for directly, e.g. in the decay modes $H \rightarrow hh$ and $A \rightarrow Zh$, where the properties of h are assumed to be

Table 2: Coupling scale factors of the neutral CP-even Higgs boson h for the four 2HDM types. For a SM-like h boson, all coupling scale factors are equal to 1.

Coupling scale factor	Type I	Type II	Type III	Type IV
κ_V	$\sin(\beta - \alpha)$	$\sin(\beta - \alpha)$	$\sin(\beta - \alpha)$	$\sin(\beta - \alpha)$
κ_u	$\cos(\alpha)/\sin(\beta)$	$\cos(\alpha)/\sin(\beta)$	$\cos(\alpha)/\sin(\beta)$	$\cos(\alpha)/\sin(\beta)$
κ_d	$\cos(\alpha)/\sin(\beta)$	$-\sin(\alpha)/\cos(\beta)$	$\cos(\alpha)/\sin(\beta)$	$-\sin(\alpha)/\cos(\beta)$
κ_ℓ	$\cos(\alpha)/\sin(\beta)$	$-\sin(\alpha)/\cos(\beta)$	$-\sin(\alpha)/\cos(\beta)$	$\cos(\alpha)/\sin(\beta)$


Figure 6: Excluded and allowed parameter ranges in the 2HDM Type-II scenario from an interpretation of the ATLAS Higgs boson coupling strength measurements [21] (left), and from direct searches for heavy H and A Higgs bosons by CMS [21] (right).

those of the SM-like 125.6 GeV Higgs boson. The $H \rightarrow hh$ decay is preferred in the mass range $2m_h < m_H < 2m_t$, while $A \rightarrow Zh$ production would be enhanced for $m_h + m_Z < m_A < 2m_t$. CMS is analysing a rather complete set of possible final states for both decay modes, taking into account all combinations of $h \rightarrow WW^*, ZZ^*, \gamma\gamma, \tau\tau$ and $Z \rightarrow \ell\ell$ decays. This leads to complex event signatures, which are analysed separately. However, no significant excess of events is observed in data above the SM expectation [21]. The search results are therefore used to set limits on the 2HDM parameters β and α , as displayed in Figure 6. Again, the parameter range around $\cos(\beta - \alpha) = 0$ can not be excluded for any value of $\tan\beta$. Also, $\tan\beta$ values between 3 and 60 are more difficult to exclude since the Hhh coupling strength is minimal in this parameter range [20].

In a simplified version of the MSSM, the Higgs sector is a Type-II 2HDM where, moreover,

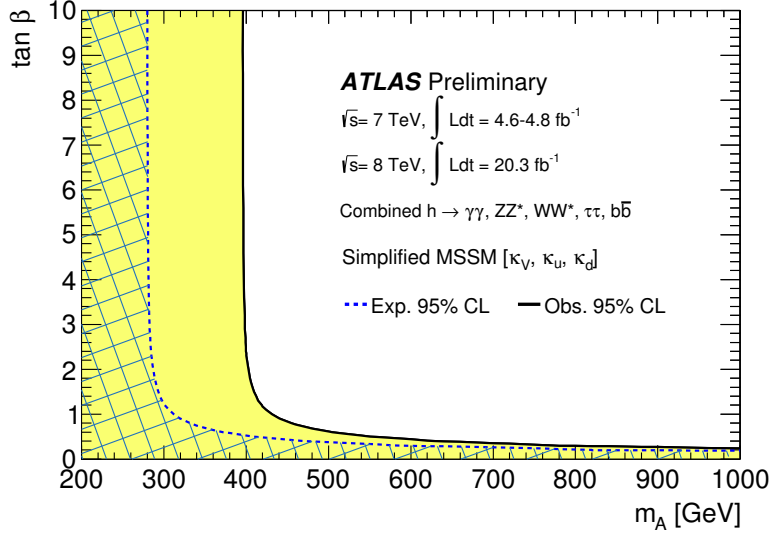


Figure 7: Excluded parameter ranges in the simplified MSSM, in which effects by supersymmetric particles are neglected in the Higgs sector, as derived by ATLAS [21].

effects of supersymmetric particles are neglected. The Higgs sector is then fully defined by the mass of the A Higgs boson and $\tan\beta$. The coupling strength measurements performed for the 125.6 GeV Higgs boson can again be used to constrain the h couplings and thus the parameter space in the m_A - $\tan\beta$ plane, as illustrated in Figure 7. In this simplified scenario, masses of the heavy Higgs bosons, $m_A \approx m_H$, less than 400 GeV can be excluded at 95% CL for $\tan\beta$ values below 10 [21].

Heavy MSSM Higgs bosons are also searched for directly by ATLAS and CMS. Here, the fact is exploited that the coupling to heavy down-type fermions, like b quarks or τ leptons, are enhanced with increasing $\tan\beta$, as e.g. indicated in Table 2. Since $H/A \rightarrow b\bar{b}$ decays are difficult to detect in the overwhelming QCD jet background at the LHC, the searches for neutral MSSM Higgs bosons mainly analyse the $H/A \rightarrow \tau^+\tau^-$ channel. The production is via gluon-gluon fusion, but also involves processes with b quarks in the final state, like $g + b \rightarrow H/A + b$ or $gg \rightarrow H/A + b\bar{b}$. The searches therefore use event categories with different number of b -jets and identify hadronic and leptonic decays of the τ leptons. In the reconstructed $m_{\tau\tau}$ mass spectrum no significant excess of data above the expected background is observed [22]. The upper limits on cross-section times branching ratio for $H/A \rightarrow \tau^+\tau^-$ production are therefore used to exclude regions in the $\tan\beta$ - m_A plane, which is shown for the CMS results in Figure 8. Also here, low m_A masses can be excluded by LHC data for $\tan\beta$ greater than 8. Currently, the so-called m_h^{\max} scenario is assumed which maximizes the mass of the lightest MSSM Higgs boson. However, this brings some tension with the observed mass of the SM-like Higgs boson of 125.6 GeV. More recently, interpretations with different mixing in the supersymmetric top sector are applied, which can relieve this tension and are still in agreement with searches for other supersymmetric particles at LHC [6, 22].

The MSSM Higgs sector also contains charged Higgs bosons, H^\pm , which couple to fermions of the same $SU(2)_L$ doublet. If the H^\pm Higgs bosons are lighter than the top quark, $m_{H^\pm} < m_t$,

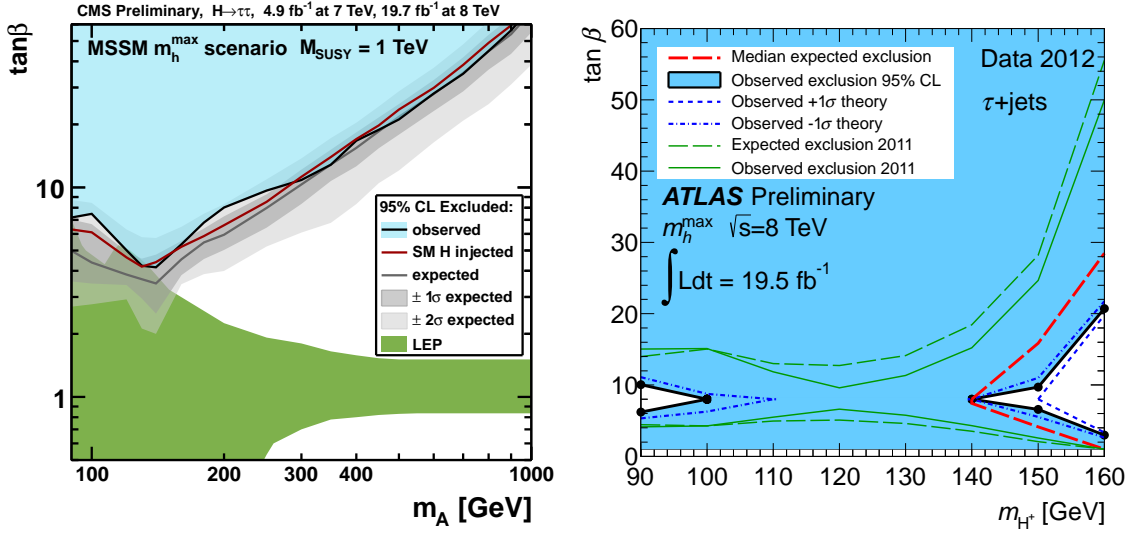


Figure 8: Left: Exclusion limits in the MSSM $\tan\beta$ - m_A parameter plane derived from direct searches by CMS for neutral MSSM Higgs bosons in the decay mode $A/H \rightarrow \tau^+\tau^-$, together with search results by LEP [22]. Right: Exclusion limits in the $\tan\beta$ - m_{H^\pm} plane derived from direct searches for light, charged MSSM Higgs bosons by ATLAS [23].

the main production mode at the LHC is through SM top-pair production and a subsequent decay $t\bar{t} \rightarrow H^\pm b + W^\mp b$. In the high-mass range, $m_{H^\pm} > m_t$, $tH^\pm(b)$ production is possible, although with a much smaller cross-section. The decay mode $H^\pm \rightarrow \tau^\pm \nu$ is preferred at large $\tan\beta$. The main idea to suppress the SM top-pair background is the enhanced number of events with τ lepton flavor compared to the SM top decays with an equal amount of leptonic $W \rightarrow \ell\nu$ final states. The hadronic decay of the tau is therefore used to identify $H^\pm b + W^\mp b$ events, together with reconstructed b -jets and the leptonic or hadronic decay of the W boson, $W \rightarrow q\bar{q}', \ell\nu$. The analysis of the reconstructed H^\pm transverse mass does not yield any significant excess of data above background. The upper limits on the branching ratio $\text{BR}(t \rightarrow bH^\pm)$ as a function of m_{H^\pm} are finally used to constrain the $\tan\beta$ - m_{H^\pm} parameter space of the MSSM Higgs sector. The results by the ATLAS experiment [23] are shown in Figure 8. For H^\pm masses of $100 \text{ GeV} < m_{H^\pm} < 140 \text{ GeV}$, the complete $\tan\beta$ range is excluded in the m_h^{max} scenario. The production cross-section is proportional to $\Gamma(H^\pm \rightarrow t) \propto m_t^2 / \tan^2\beta + m_b^2 \tan^2\beta$, which has a minimum for $\tan\beta = \sqrt{m_t/m_b} \approx 6$. The exclusion limits thus become weaker in this $\tan\beta$ range for larger and smaller m_{H^\pm} values.

5. Summary and conclusions

After analysing nearly the complete LHC Run-1 data set, the ATLAS and CMS experiments clearly observe a scalar Higgs boson with a mass of $125.6 \pm 0.4 \text{ GeV}$ [14], and a narrow width of $\Gamma_H < 22 \text{ MeV}$ [17]. The spin and CP properties are consistent with the $J^{CP} = 0^{++}$ hypothesis, and all fermionic and bosonic coupling measurements are in agreement with the SM predictions within the current measurement uncertainties. Furthermore, in the search for additional neutral or charged

Higgs bosons no significant excess of events has been observed in the data analysed until the time of the conference.

More data will be collected in the upcoming LHC Run-2, where the centre-of-mass energy will be raised to 13 – 14 TeV and the total luminosity is expected to be increased by a factor 4-5 with respect to Run-1. This will allow an improved determination of the Higgs boson properties. Measurements of rare Higgs boson production and decay modes may come into reach, like associated $t\bar{t}H$ production and $H \rightarrow \mu^+\mu^-$, $H \rightarrow Z\gamma$, $H \rightarrow \gamma\gamma^*$ decays. The Higgs sector in theories beyond the Standard Model will be also tested further. In particular, the searches will be extended to non-Minimal Supersymmetric Models and to general 2HDM or effective field theory interpretations. The LHC will thus continue to probe elementary physics at TeV energies and will verify if New Physics is realised at these energy scales.

Acknowledgments

This work was supported in part by the German Bundesministerium für Bildung und Forschung (BMBF) within the research network FSP-101 *Physics on the TeV Scale with ATLAS at the LHC*.

References

- [1] Evans, L., Bryant, Ph. (eds.), *LHC Machine*, JINST **3** (2008) S08001.
- [2] ATLAS Collaboration, JINST **3** (2008) S08003.
- [3] CMS Collaboration, JINST **3** (2008) S08004.
- [4] S.L. Glashow, Nucl. Phys. **22** (1961) 579; S. Weinberg, Phys. Rev. Lett. **19** (1967) 1264; A. Salam, *Elementary Particle Theory*, Ed. N. Svartholm, Stockholm, *Almqvist and Wiksell*, 1968, p. 367; G. t’Hooft, Nucl. Phys. **B 35** (1971) 167; G. t’Hooft and M. Veltman, Nucl. Phys. **B 44** (1972) 189; P.W. Higgs, Phys. Lett. **12** (1964) 132; *idem*, Phys. Rev. Lett. **13** (1964) 508; *idem*, Phys. Rev. **145** (1966) 1156; F. Englert and R. Brout, Phys. Rev. Lett. **13** (1964) 321; G.S. Guralnik, C.R. Hagen and T.W.B. Kibble, Phys. Rev. Lett. **13** (1964) 585; H. Fritzsch, M. Gell-Mann, H. Leutwyler, Phys. Lett. **B 47** (1973) 365; H. D. Politzer, Phys. Rev. Lett. **30** (1973) 1346; D. Gross, F. Wilczek, Phys. Rev. Lett. **30** (1973) 1343; S. Weinberg, Phys. Rev. Lett. **31** (1973) 494.
- [5] ATLAS Collaboration, Phys. Lett. B 716 (2012) 1; CMS Collaboration, Phys. Lett. B 716 (2012) 30.
- [6] The LHC Higgs Cross Section Working Group, *Handbook of LHC Higgs cross sections*, arXiv:1101.0593, arXiv:1201.3084, arXiv:1307.1347.
- [7] ATLAS Collaboration, Phys. Lett. B 726 (2013) 88; CMS Collaboration, Phys. Rev. D 89 (2014) 092007, JHEP 01 (2014) 096, CMS PAS HIG-13-001.
- [8] ATLAS Collaboration, Conference Note ATLAS-CONF-2013-108; CMS Collaboration, JHEP 05 (2014) 104.
- [9] ATLAS Collaboration, Conference Note ATLAS-CONF-2014-009; CMS Collaboration, Physics Analysis Note CMS-PAS-HIG-13-005.
- [10] ATLAS Collaboration, Conference Notes ATLAS-CONF-2014-011, ATLAS-CONF-2013-080; CMS Collaboration, Physics Analysis Notes CMS-PAS-HIG-12-025, CMS-PAS-HIG-13-015, CMS-HIG-13-019, CMS-PAS-HIG-13-020.

- [11] L. D. Landau, Dokl. Akad. Nauk., USSR 60 (1948) 207; C. N. Yang, Phys. Rev. 77 (1950) 242.
- [12] see e.g.: T. Hastie, R. Tibshirani, and J. Friedman, “The Elements of Statistical Learning”, 2nd ed., Springer (2009), and references therein.
- [13] ATLAS Collaboration, Phys. Lett. B 726 (2013) 120; CMS Collaboration, Phys. Rev. D 89 (2014) 092007.
- [14] K.A. Olive et al. (Particle Data Group), Chin. Phys. C, 38, 090001 (2014).
- [15] ATLAS Collaboration, Conference Note ATLAS-CONF-2013-014; CMS Collaboration, Physics Analysis Note CMS-PAS-HIG-13-005.
- [16] J. M. Campbell, R. K. Ellis, C. Williams, “Bounding the Higgs width at the LHC using full analytic results for $gg \rightarrow 2e2\mu$ ”, FERMILAB-PUB-13-508-T, arXiv:1311.3589.
- [17] CMS Collaboration, Phys. Lett. B 736 (2014) 64.
- [18] ATLAS Collaboration, Phys. Rev. Lett. 112 (2014) 201802, ATLAS-CONF-2014-010; CMS Collaboration Eur. Phys. J. C 74 (2014) 2980, CMS-HIG-13-018, CMS-HIG-13-028, CMS-HIG-13-013.
- [19] P. Langacker, Phys. Rep. 72 (1981) 185.
- [20] see e.g.: G. C. Branco, P. M. Ferreira, L. Lavoura, M. N. Rebelo, M. Sher, J. P. Silva, Phys. Rept. 516 (2012) 1; A. Djouadi, Phys. Rept. 457 (2008) 1.
- [21] ATLAS Collaboration, Conference Note ATLAS-CONF-2014-010; CMS Collaboration, Physics Analysis Note, CMS-PAS-HIG-13-025.
- [22] ATLAS Collaboration, JHEP 02 (2013) 095; CMS Collaboration, Phys. Lett. B 722 (2013) 207, Physics Analysis Note CMS-HIG-13-021
- [23] ATLAS Collaboration, Eur. Phys. J. C, 73 6 (2013) 2465, JHEP 03 (2013) 076, ATLAS-CONF-2013-090.